 CMES, vol.8, no.1, pp.45-59, 2005

A new free energy-based model of the kinematic hardening in large strain elastoplasticity

Igor Karšaj[1] **,Carlo Sansour**[2] **and Jurica Sorić**[1]

Abstract: In this paper, a free energy-based formulation incorporating the effect of kinematic hardening is proposed. The formulation is able to reproduce symmetric expressions for the back stress while incorporating the multiplicative decomposition of the deformation gradient. Kinematic hardening is combined with isotropic hardening where an associative flow rule and von Mises yield criterion are applied. An accurate and trivial wise objective integration algorithm employing the exponential map is developed. In order to ensure a high convergence rate in the global iteration approach, an algorithmic tangent operator is derived. The computational algorithm is implemented and applied to a shell finite element which allows the use of complete three-dimensional constitutive laws. Robustness and efficiency of the proposed algorithm are demonstrated by numerical examples.

keyword: large strains; elastoplasticity; free energy; kinematic hardening; isotropic hardening

1 Introduction

Inelastic structural responses and their numerical simulation have been attracting increasing attention in recent years. A more realistic material modelling demands consideration of sophisticated constitutive models in finite strain plasticity, where kinematic hardening is employed. The combined isotropic-kinematic hardening model has been considered in the available literature from different viewpoints (e.g. Atluri (1984b), Dogui and Sidoroff (1985), Im and Atluri (1987), Eterovic and Bathe (1990), Wang and Atluri (1994) , Papadopoulos and Lu (1997), Başar and Itskov (1999), Sorić, Skoko, and Eckstein (2002), Tsakmakis and Willuweit (2004)). Kinematic hardening is usually described by a so-called back stress, which is considered as an internal variable and for which adequate constitutive equations must be formulated.

The extension of small strain formulations to the large strain case, in the presence of the back stress, is by no means trivial and calls for particular attention. In the large strain case the theoretical development is naturally carried out in a material framework. Evolution equations in terms of material time derivatives result, however, in a back stress tensor which is not symmetric once pushed-forward to the actual configuration; suggesting that the formulation is flawed. Expressions for symmetric back stress can be obtained by considering the stress at the actual configuration (Cauchy-like or Kirchhoff-like back stress tensor). In this case the evolution equation for the back stress necessarily employs the notion of objective rate.

A simple model for the evolution of the kinematic hardening variable in a rate-type material model has been presented in Reed and Atluri (1985). An objective numerical integration scheme is proposed and discussed. Other attempts to derive a numerically efficient integration algorithm employing an objective rate of the hardening variable may be found in (e.g. Eterovic and Bathe (1990), Papadopoulos and Lu (1997), Tsakmakis (1996), Tsakmakis and Willuweit (2004)). Beyond the fact that a variety of objective rates exist, with no clear evidence as to which one is the appropriate choice and with some, as the Zaremba-Jaumann one, producing oscillatory responses, the numerical effort in time-integration is considerable.

On the other hand, it is well known that in the small strain regime (linear theory) the back stress can be efficiently derived from an extended form of the stored energy function (see e.g. Nguyen (1993)). Essentially the inelastic part of the additively decomposed strain is included in the free energy function. A novel contribution of this paper is the formulation of an extended form of the free energy which incorporates the effect of kinematic hardening in the large strain regime. The formulation enjoys

[1] Faculty of Mechanical Engineering and Naval Architecture, University of Zagreb, I.Lučića 5, HR-10000 Zagreb, Croatia

[2] The University of Adelaide, School of Mechanical Engineering, SA 5005, Australia

the features of reproducing symmetric expressions for the back stress (at the actual configuration) and of incorporating the multiplicative decomposition of the deformation gradient. The constitutive model is developed and established at the spatial configuration and then reformulated in a material setting. While formulations at the current configuration allow for more insight into obtaining a symmetric back stress, from a numerical point of view it is more appropriate to deal with the reference configuration. A further advantage of a material setting lies in its ability to handle anisotropic material laws, allowing for possible extension in the future. The kinematic hardening is combined with isotropic hardening, where an associative flow rule and von Mises yield criterion are applied.

Several stress and work-conjugate strain measures for analysis of large deformation responses are discussed in Atluri (1984a). For the first time the rotated Cauchy stress tensor is suggested as work conjugate stress to the logarithmic strain. Later, a logarithmic strain measure was successfully used (e.g. Eterovic and Bathe (1990), Perić, Owen, and Honnor (1992), Rouainia and Perić (1998), Sansour and Kollmann (1998), Sansour and Wagner (2003)). It has proven to be very efficient as it allows for almost additive structures within the numerical treatment, in spite of the fact that the formulation can be based on the multiplicative decomposition of the deformation gradient. However, an approach based on the logarithm of the elastic strain tensor exhibits some disadvantages. First, the approach is based on the assumption of isotropy of the constitutive law and can't be further extended to anisotropy. Second, even if the energy is chosen to be quadratic in the logarithmic strain tensor, it is not an elliptic function at very large deformations. As the present formulation is to be extended in the future to deal with anisotropic inelasticity, the elastic part of the energy is formulated in terms of the elastic right Cauchy-Green tensor itself, as has already been dealt with in Sansour and Wagner (2001). A result of such a choice is that the expression for the algorithmic tangent operator becomes very complex and the symmetry of the operator is generally lost.

For integration of constitutive equations the predictor-corrector schemes employing the exponential map have mostly been used (e.g. Eterovic and Bathe (1990), Başar and Itskov (1999), Sansour and Wagner (2001)). An alternative computational strategy for integration of the constitutive model of convex plasticity has recently been proposed in Liu and Chang (2004). However their model is restricted to small strain plasticity as well as perfectly plastic materials. In this paper an accurate and automatically objective integration algorithm employing the exponential map is developed. The use of the exponential map method was first suggested in Eterovic and Bathe (1990) for symmetric arguments and then extended to non-symmetric arguments in Sansour and Kollmann (1998) and Sansour and Wagner (2001).

The theory and the computational algorithms have been implemented and applied to a shell finite element developed in Sansour and Kollmann (1998) and Sansour and Wagner (2001). The shell formulation allows for the use of complete three-dimensional constitutive laws. Robustness and efficiency of the proposed algorithms are demonstrated by numerical examples.

The paper is organized as follows. In Section 2 kinematics of the elastic-inelastic body are reviewed. In Section 3 the constitutive framework is fully developed. The theory is formulated at the current configuration using spatial quantities which are then pulled-back to the reference configuration to produce the material counterpart of the spatial formulation. Section 4 is devoted to the numerical treatment and is divided into two subsections. While the first subsection presents the local integration algorithm, the second considers the derivation of the consistent elastoplastic tangent operator. In Section 5 various numerical examples are presented. The paper closes with some conclusions.

2 Kinematics of the elastic-inelastic body

In this section the fundamental kinematic relations are summarized briefly and appropriate notation is introduced. Let $B \subset \mathbb{R}^3$ define a body. A motion of the body B is represented by a one-parameter mapping $\varphi : B \longrightarrow B_t$, where $t \in \mathbb{R}$ is the time (or time-like) and B_t is the current configuration at time t. We assume that the body can be identified with its configuration at time $t = 0$, which we refer to as the reference configuration. That is φ_o is the identity map, At the reference configuration, every material point is associated with the position vector $\mathbf{X} \in B$ and at the current configuration with $\mathbf{x} \in B_t$. Thus, the relation holds $\varphi : \varphi(\mathbf{X}) = \mathbf{x}$. The tangent map related to φ is the deformation gradient $\mathbf{F}$ which maps the tangent space $T_X B$ at the reference configuration to the tangent space $T_x B_t$ at the actual configuration,

$\mathbf{F} := T_X B \longrightarrow T_x B_t$. The deformation gradient is a two-point tensor.

For the description of the inelastic deformation, the well established multiplicative decomposition of the deformation gradient in an elastic part, $\mathbf{F_e}$, and an inelastic part, $\mathbf{F_p}$, is assumed:

$$\mathbf{F} = \mathbf{F_e}\mathbf{F_p}. \tag{1}$$

For metals, the inelastic part is accompanied by the assumption $\mathbf{F_p} \in SL^+(3,\mathbb{R})$ which reflects the incompressibility of the inelastic deformations, where $SL^+(3,\mathbb{R})$ denotes the special linear group with determinants equal to one.

On the basis of the decomposition (1), the following left Cauchy-Green-type tensors (formulated at the current configuration) are defined:

$$\mathbf{b} = \mathbf{F}\mathbf{F}^{\mathrm{T}}, \tag{2}$$

$$\mathbf{b_e} = \mathbf{F_e}\mathbf{F_e}^{\mathrm{T}}, \tag{3}$$

where $\mathbf{b_e}$ is to be understood as the elastic deformation tensor. Correspondingly, right Cauchy-Green-type tensors can be defined as follows

$$\mathbf{C} = \mathbf{F}^{\mathrm{T}}\mathbf{F}, \tag{4}$$

$$\mathbf{C_e} = \mathbf{F_e}^{\mathrm{T}}\mathbf{F_e}, \tag{5}$$

$$\mathbf{C_p} = \mathbf{F_p}^{\mathrm{T}}\mathbf{F_p}, \tag{6}$$

where $\mathbf{C_e}$ is an elastic tensor and $\mathbf{C_p}$ is its analogous plastic counterpart.

Understanding the deformation gradient $\mathbf{F}$ as an element of the general linear group $GL^+(3,\mathbb{R})$, linear transformations with positive determinant, it becomes natural to define left and right time derivatives as follows

$$\dot{\mathbf{F}} = \mathbf{l}\mathbf{F}, \tag{7}$$

$$\dot{\mathbf{F}} = \mathbf{F}\mathbf{L}, \tag{8}$$

where $\mathbf{l}$ is the left and $\mathbf{L}$ is the right rate, respectively. Both rates are mixed-variant tensors. In accordance with (7) and (8) the following relation follows

$$\mathbf{L} = \mathbf{F}^{-1}\mathbf{l}\mathbf{F}. \tag{9}$$

$\mathbf{L}$ is thus the pull-back of the mixed velocity gradient from the current configuration to the reference configuration. Since $\mathbf{F_p} \in SL^+(3,\mathbb{R})$, here too a left and a right rate of the inelastic part of the deformation gradient can be defined. The same is true for $\mathbf{F_p}$. We consider the following rates

$$\dot{\mathbf{F}}_\mathbf{e} = \mathbf{l_e}\mathbf{F_e}, \tag{10}$$

$$\dot{\mathbf{F}}_\mathbf{p} = \mathbf{F_p}\mathbf{L_p}. \tag{11}$$

Taking Eq. (7) into consideration we get immediately

$$\mathbf{l} = \mathbf{l_e} + \mathbf{F}\mathbf{L_p}\mathbf{F}^{-1}, \tag{12}$$

which establishes the mixed-variant push-forward of the material inelastic rate $\mathbf{L_p}$ according to

$$\mathbf{l_p} = \mathbf{F}\mathbf{L_p}\mathbf{F}^{-1}\,, \tag{13}$$

as the spatial inelastic rate. The relation holds

$$\mathbf{l} = \mathbf{l_e} + \mathbf{l_p}\,, \tag{14}$$

which supports the transformation rule formulated in Eq. (13).

3 Constitutive relations

3.1 New approach, free energy function, and reduced dissipation

We assume that the elastic behaviour of the body is fully characterized by means of a free energy function $\psi\theta bal$. This function will depend on the measure of elastic strains and on further sets of internal variables which are expected to capture certain physical features of the micro structure of the material and transfer it to the macro level. These internal variables can be of scalar as well as of tensorial nature. We consider isotropic hardening to be characterized by the scalar quantity Z, while kinematical hardening is supposed to relate to a tensorial strain-like quantity of second order, which we denote by $\mathbf{b_q}$. Accordingly, we assume the existence of a free energy function $\psi(\mathbf{b_e}, \mathbf{b_q}, Z)$, where $\mathbf{b_e}$ and $\mathbf{b_q}$ are strain-like tensors defined at the actual configuration. While the definition of $\mathbf{b_e}$ is clear from (3), an adequate definition for $\mathbf{b_q}$ remains to be found. Ad-hoc choices fail to ensure the symmetry of the back stress. What we need is an appropriate inelastic quantity which is defined at the current configuration. A natural choice would be a push-forward of $\mathbf{F_p}$, or $\mathbf{F_p}^{-1}$ to the current configuration. A natural choice is to accomplish this transformation in a mixed variant manner. Taking a look at Eq. (13), which

relates the material rate $\mathbf{L_p}$ to the spatial one, it becomes obvious that the mixed variant transformation is rather natural and is inherent in the structure of the theory. First we define a spatial inelastic tensor as

$$\mathbf{f_p} = \mathbf{F}\mathbf{F_p}^{-1}\mathbf{F}^{-1}. \tag{15}$$

We first note that $\mathbf{f_p}$ is an objective tensor. Then, for any $\mathbf{R} \in SO(3)$ (that is $\mathbf{R}$ is a rotation tensor) superimposed on $\mathbf{F}$, we have the modified deformation gradient

$$\tilde{\mathbf{F}} = \mathbf{R}\mathbf{F}. \tag{16}$$

The $\mathbf{f_p}$ transfers now according to

$$\begin{aligned}\tilde{\mathbf{f}}_\mathbf{p} =& \mathbf{R}\mathbf{F}\mathbf{F}_\mathbf{p}^{-1}\mathbf{F}^{-1}\mathbf{R}^{\mathrm{T}} \\ =& \mathbf{R}\mathbf{f_p}\mathbf{R}^{\mathrm{T}},\end{aligned} \tag{17}$$

which is nothing but the transformation rule of an objective tensor. Note also that $\mathbf{F_p}$ is treated as a material tensor invariant under rigid body motion.

Having established a spatial inelastic quantity, we choose $\mathbf{b_q}$ to be of the form

$$\mathbf{b_q} = \mathbf{f_p}\mathbf{f_p}^{\mathrm{T}} \tag{18}$$

The choice is natural and follows the same lines as in the definition of $\mathbf{b_e}$. It will be shown that it provides us with appropriate and symmetric forms for the back stress.

Further, we assume the free energy to be decomposed into an elastic part, $\psi_e(\mathbf{b_e})$, and further plastic parts. The latter are the sum of a part depending on the kinematic hardening, $\psi_q(\mathbf{b_q})$, and a part depending on the isotropic hardening, $\psi_Z(Z)$. Thus, we have

$$\begin{aligned}\psi =& \psi^{elastic} + \psi^{plastic} \\ \psi =& \psi_e(\mathbf{b_e}) + \psi_q(\mathbf{b_q}) + \psi_Z(Z)\end{aligned} \tag{19}$$

Having identified the free energy function, the evaluation of the dissipation inequality

$$D = \boldsymbol{\tau} : \mathbf{l} - \rho_0 \dot{\psi}(\mathbf{b_e}, \mathbf{b_q}, Z), \tag{20}$$

follows. The evaluation of Eq. (20) first gives

$$D = \boldsymbol{\tau} : \mathbf{l} - \rho_0 \frac{\partial \psi}{\partial \mathbf{b_e}} : \dot{\mathbf{b}}_\mathbf{e} - \rho_0 \frac{\partial \psi}{\partial \mathbf{b_q}} : \dot{\mathbf{b}}_\mathbf{q} - \rho_0 \frac{\partial \psi}{\partial Z} \cdot \dot{Z} \geq 0. \tag{21}$$

Using Eqs. (1), (3), (6), (7), (11), (15), and (18), the time derivatives of $\mathbf{b_e}$ and $\mathbf{b_q}$ read

$$\dot{\mathbf{b}}_\mathbf{e} = \mathbf{l}\mathbf{b_e} - \mathbf{l_p}\mathbf{b_e} - \mathbf{b_e}\mathbf{l}_\mathbf{p}^{\mathrm{T}} + \mathbf{b_e}\mathbf{l}^{\mathrm{T}}, \tag{22}$$

$$\dot{\mathbf{b}}_\mathbf{q} = \mathbf{l}\mathbf{b_q} + \mathbf{b_q}\mathbf{l}^{\mathrm{T}} - \mathbf{f_p}(\mathbf{l}+\mathbf{l}^{\mathrm{T}})\mathbf{f}_\mathbf{p}^{\mathrm{T}} - \mathbf{l_p}\mathbf{b_q} - \mathbf{b_q}\mathbf{l}_\mathbf{p}^{\mathrm{T}}. \tag{23}$$

By assuming that the functions are isotropic and by inserting (22) and (23) in (21), we are provided with

$$\begin{aligned}D = &\left(\boldsymbol{\tau} - 2\rho_0 \frac{\partial \psi}{\partial \mathbf{b_e}}\mathbf{b_e} - 2\rho_0 \frac{\partial \psi}{\partial \mathbf{b_q}}\mathbf{b_q} + 2\rho_0 \mathbf{f}_\mathbf{p}^{\mathrm{T}} \frac{\partial \psi}{\partial \mathbf{b_q}}\mathbf{f_p}\right) : \mathbf{l} + \\ &\left(2\rho_0 \frac{\partial \psi}{\partial \mathbf{b_e}}\mathbf{b_e} + 2\rho_0 \frac{\partial \psi}{\partial \mathbf{b_q}}\mathbf{b_q}\right) : \mathbf{l_p} - \rho_0 \frac{\partial \psi}{\partial Z} \cdot \dot{Z} \geq 0.\end{aligned} \tag{24}$$

Assuming now that Eq. (24) has to hold for all possible processes, it is a classical argument of thermodynamics to infer then that the following relations have to hold

$$\boldsymbol{\tau} = 2\rho_0 \frac{\partial \psi}{\partial \mathbf{b_e}}\mathbf{b_e} + 2\rho_0 \frac{\partial \psi}{\partial \mathbf{b_q}}\mathbf{b_q} - 2\rho_0 \mathbf{f}_\mathbf{p}^{\mathrm{T}} \frac{\partial \psi}{\partial \mathbf{b_q}}\mathbf{f_p}, \tag{25}$$

$$D_r = \left(2\rho_0 \frac{\partial \psi}{\partial \mathbf{b_e}}\mathbf{b_e} + 2\rho_0 \frac{\partial \psi}{\partial \mathbf{b_q}}\mathbf{b_q}\right) : \mathbf{l_p} - \rho_0 \frac{\partial \psi}{\partial Z} \cdot \dot{Z} \geq 0\,. \tag{26}$$

With the definitions

$$Y = -\rho_0 \frac{\partial \psi}{\partial Z}, \tag{27}$$

and

$$\boldsymbol{\gamma} = 2\rho_0 \frac{\partial \psi}{\partial \mathbf{b_e}}\mathbf{b_e} + 2\rho_0 \frac{\partial \psi}{\partial \mathbf{b_q}}\mathbf{b_q}, \tag{28}$$

Eq. (26) takes the form

$$D_r = \boldsymbol{\gamma} : \mathbf{l_p} + Y \cdot \dot{Z} \geq 0, \tag{29}$$

Accordingly, Y is the conjugate variable to the internal variable Z and $\boldsymbol{\gamma}$ is the relative stress, which acts as the conjugate variable of the inelastic rate $\mathbf{l_p}$. Since the relative stress must be of the form

$$\boldsymbol{\gamma} = \boldsymbol{\tau} - \mathbf{q}, \tag{30}$$

where $\mathbf{q}$ is again the back stress, we conclude

$$\mathbf{q} = -2\rho_0 \mathbf{f}_\mathbf{p}^{\mathrm{T}} \frac{\partial \psi}{\partial \mathbf{b_q}}\mathbf{f_p} \tag{31}$$

as the corresponding expression for it. It is obvious that $\mathbf{q}$ retains symmetry. A basic advantage of the above expressions is already apparent from Eq. (31). The back stress tensor can be explicitly calculated, avoiding the need to formulate and integrate an objective rate as in Eterovic and Bathe (1990), Sorić, Skoko, and Eckstein (2002), Tsakmakis (1996). It should be mentioned that the expression for the back stress itself may depend on further

internal variables. This is especially true if one is interested in modelling the saturation phenomenon. However, these extra internal variables will be of scalar nature and will not diminish the above mentioned advantage.

Now, in accordance with the usual expressions in the literature (e.g. Perić, Owen, and Honnor (1992), Simo (1988), Tsakmakis and Willuweit (2004)), the elastic free energy is assumed to be of the following form

$$\psi_e = \frac{1}{2}\alpha_1 \left(\mathrm{tr}(\mathbf{b_e}-\mathbf{1})\right)^2 + \frac{1}{2}\alpha_2 \mathrm{tr}(\mathbf{b_e}-\mathbf{1})^2 \quad , \tag{32}$$

where α_1 and α_2 define the elastic constants. The part of the free energy related to the kinematic hardening is assumed to be of the form

$$\psi_q = \frac{1}{2}\, c\, \mathrm{tr}\, \tilde{\mathbf{b}}_\mathbf{q}, \tag{33}$$

where c is the kinematic hardening parameter and the definition also holds

$$\tilde{\mathbf{b}}_\mathbf{q} = \frac{\mathbf{b_q}}{(\det \mathbf{b_q})^{1/3}}. \tag{34}$$

The choice of ψ_q is dictated by the physical requirements, generally accepted to be valid in metal plasticity, namely $\mathrm{tr}\,\mathbf{q} = 0$.

Altogether, and with (32) and (33), $\boldsymbol{\gamma}$ and $\mathbf{q}$ can be expressed as

$$\begin{aligned}\boldsymbol{\gamma} = {} & 2\rho_0 \left(\alpha_1 \mathrm{tr}(\mathbf{b_e}-\mathbf{1})\mathbf{b_e} + \alpha_2(\mathbf{b_e}-\mathbf{1})\mathbf{b_e}\right) \\ & + \rho_0 \frac{c}{(\det \mathbf{b_q})^{1/3}}\, \mathrm{dev}(\mathbf{b_q}),\end{aligned} \tag{35}$$

$$\mathbf{q} = -\rho_0 \frac{c}{(\det \mathbf{f_p})^{2/3}}\, \mathrm{dev}(\mathbf{f_p^T f_p})\,, \tag{36}$$

where dev denotes the deviator. It should be noted that the constitutive law for the back stress is not linear in the quantity $\mathbf{b_q}$. However, the present form is certainly a simplification. In this paper we confine ourselves to this simple form. More sophisticated laws, which include saturation effects may be developed as well. However, such a task is left for future work.

3.2 Evolution equations and inelastic behaviour

We turn our attention now to the description of the inelastic behaviour. The existence of a purely elastic domain E described by means of a convex yield function ϕ expressed in terms of the Kirchhoff stress tensor $\boldsymbol{\tau}$ and the conjugate variables of the internal variables is assumed:

$$E := \{(\boldsymbol{\tau}, \mathbf{q}, Y) : \phi(\boldsymbol{\tau}, \mathbf{q}, Y) \leq 0\}. \tag{37}$$

As usual for metal plasticity, the von Mises yield function is assumed, written in the following form:

$$\phi = \| \,\mathrm{dev}\, \boldsymbol{\gamma}\, \| - \sqrt{\frac{2}{3}}\,(\sigma_Y - Y)\,. \tag{38}$$

Here, σ_Y denotes the initial yield stress, $\| \,\mathrm{dev}\, \boldsymbol{\gamma}\, \|$ is the norm of the relative stress deviator; we recall

$$\mathrm{dev}\, \boldsymbol{\gamma} = \mathrm{dev}\, \boldsymbol{\tau} - \mathrm{dev}\, \mathbf{q}. \tag{39}$$

In addition, the following form for Y is assumed:

$$Y = -HZ - (\sigma_\infty - \sigma_Y) \cdot (1 - \exp(-\eta Z))\,,$$

where H is a linear isotropic hardening parameter and σ_∞ the saturation yield stress, while η is a constitutive parameter quantifying the rate at which the saturation yield stress is attained during loading.

To derive evolution equations for the internal variables we rely on the principle of maximum dissipation which leads to the classical variational equation

$$\int \left(-\left(\boldsymbol{\gamma} : \mathbf{l_p} + Y \cdot \dot{Z}\right) + \lambda \phi(\boldsymbol{\gamma}, Y)\right) ds = stat. \tag{40}$$

Herein, λ denotes a plastic multiplier and ds denotes an adequately defined parameterization of the deformation path. The variational statement leads to the following associative evolution equations for the plastic strain rate and the isotropic hardening variable

$$\mathbf{l_p} = \lambda \frac{\partial \phi}{\partial \boldsymbol{\gamma}}, \tag{41}$$

$$\dot{Z} = \lambda \frac{\partial \phi}{\partial Y}. \tag{42}$$

The equations are complemented with the loading/unloading conditions in Kuhn-Tucker form

$$\lambda \geq 0\,, \qquad \lambda\, \phi(\boldsymbol{\gamma}, Y) = 0\,, \qquad \phi(\boldsymbol{\gamma}, Y) \leq 0\,, \tag{43}$$

and the consistency condition

$$\lambda \dot{\phi}(\boldsymbol{\gamma}, Y) = 0. \tag{44}$$

With the use of equations (38), (41) and (42) we end up with evolution equations in the following form

$$\mathbf{l_p} = \lambda \frac{\mathrm{dev}\, \boldsymbol{\gamma}}{\| \,\mathrm{dev}\, \boldsymbol{\gamma}\, \|}, \tag{45}$$

$$\dot{Z} = \sqrt{\frac{2}{3}}\lambda. \tag{46}$$

These equations, together with the definition of the free energy function, complete the formulation of the constitutive theory. However, from a numerical point of view, it is worthwhile to reformulate the equations, without altering the physical content, in a purely material setting, which is done next.

3.3 Material Form of the Theory

The theory is now reformulated in a purely material setting. For that purpose all equations and variables are pulled back to the reference configuration. In general, for any stress-like quantity defined at the current configuration, say $\boldsymbol{\pi}$, the transformation takes the form

$$\boldsymbol{\Pi} = \mathbf{F}^{\mathrm{T}}\boldsymbol{\pi}\mathbf{F}^{-\mathrm{T}}. \tag{47}$$

The quantity $\boldsymbol{\Pi}$ defines a material tensor. Following this transformation rule we generate the following quantities

$$\boldsymbol{\Xi} = \mathbf{F}^{\mathrm{T}}\boldsymbol{\tau}\,\mathbf{F}^{-\mathrm{T}}, \tag{48}$$

$$\boldsymbol{\Gamma} = \mathbf{F}^{\mathrm{T}}\boldsymbol{\gamma}\,\mathbf{F}^{-\mathrm{T}}, \tag{49}$$

$$\mathbf{Q} = \mathbf{F}^{\mathrm{T}}\mathbf{q}\mathbf{F}^{-\mathrm{T}}. \tag{50}$$

$\boldsymbol{\Xi}$ defines a quantity, which up to a sign and a spherical part coincides with Eshelby's stress tensor (Maugin (1994), Sansour (2001)). $\boldsymbol{\Gamma}$ is a material relative stress defined at the reference configuration and $\mathbf{Q}$ is a material back stress, where the relation holds

$$\boldsymbol{\Gamma} = \boldsymbol{\Xi} - \mathbf{Q}. \tag{51}$$

It should be mentioned that the transformation is very much motivated by the validity of the relation

$$\boldsymbol{\tau} : \mathbf{l} = \boldsymbol{\Xi} : \mathbf{L}, \tag{52}$$

with $\mathbf{L}$ being defined in (9). It should also be noted that the treatment of the stress tensors as mixed-variant quantities is fundamental if one is to arrive at correct form of the material version of the theory.

In the reference configuration the evolution equations (41) and (42) take the form

$$\mathbf{L}_{\mathbf{p}} = \lambda\frac{\operatorname{dev}\boldsymbol{\Gamma}^{\mathrm{T}}}{\parallel \operatorname{dev}\boldsymbol{\Gamma}\parallel} = \lambda\boldsymbol{\nu}, \tag{53}$$

$$\dot{Z} = \sqrt{\frac{2}{3}}\lambda \qquad , \tag{54}$$

where $\boldsymbol{\nu}$ is normal to the yield surface. The yield function (38) has the physically equivalent form

$$\phi = \parallel \operatorname{dev}\boldsymbol{\Gamma}\parallel - \sqrt{\frac{2}{3}}(\sigma_Y + Y) = 0. \tag{55}$$

The relative stress (35) and the back stress (36) are now functions of the quantities $\mathbf{C}\mathbf{C}_{\mathbf{p}}^{-1}$, $\mathbf{F}_{\mathbf{p}}^{-1}$ and $\mathbf{C}$:

$$\boldsymbol{\Gamma} = \rho_0\Big[2\alpha_1\operatorname{tr}(\mathbf{C}\mathbf{C}_{\mathbf{p}}^{-1}-\mathbf{1})\mathbf{C}\mathbf{C}_{\mathbf{p}}^{-1} + 2\alpha_2(\mathbf{C}\mathbf{C}_{\mathbf{p}}^{-1}-\mathbf{1})\mathbf{C}\mathbf{C}_{\mathbf{p}}^{-1} + \frac{c}{(\det\mathbf{F}_{\mathbf{p}}^{-1})^{2/3}}\operatorname{dev}\left(\mathbf{C}\mathbf{F}_{\mathbf{p}}^{-\mathbf{1}}\mathbf{C}^{-\mathbf{1}}\mathbf{F}_{\mathbf{p}}^{-\mathrm{T}}\right)\Big], \tag{56}$$

$$\mathbf{Q} = -\rho_0\frac{c}{(\det\mathbf{F}_{\mathbf{p}}^{-1})^{2/3}}\operatorname{dev}\left(\mathbf{F}_{\mathbf{p}}^{-\mathrm{T}}\mathbf{C}\mathbf{F}_{\mathbf{p}}^{-\mathbf{1}}\mathbf{C}^{-\mathbf{1}}\right). \tag{57}$$

With an intention of making the numerical procedures more clear, we decompose the relative stress into an 'elastic', $\boldsymbol{\Gamma}^{el.}$, and a 'plastic' part, $\boldsymbol{\Gamma}^{pl.}$, where we have

$$\boldsymbol{\Gamma}^{el.} = 2\rho_0\alpha_1\operatorname{tr}(\mathbf{C}\mathbf{C}_{\mathbf{p}}^{-1}-\mathbf{1})\mathbf{C}\mathbf{C}_{\mathbf{p}}^{-1} + 2\rho_0\alpha_2(\mathbf{C}\mathbf{C}_{\mathbf{p}}^{-1}-\mathbf{1})\mathbf{C}\mathbf{C}_{\mathbf{p}}^{-1}, \tag{58}$$

$$\boldsymbol{\Gamma}^{pl.} = \rho_0\frac{c}{(\det\mathbf{F}_{\mathbf{p}}^{-1})^{2/3}}\operatorname{dev}\left(\mathbf{C}\mathbf{F}_{\mathbf{p}}^{-1}\mathbf{C}^{-1}\mathbf{F}_{\mathbf{p}}^{-\mathrm{T}}\right), \tag{59}$$

as the corresponding explicit expressions.

4 Numerical formulation

4.1 Time integration

Integration of the evolution equations is performed by using the well-known predictor-corrector computational strategy. After updating the state variable at time t_n, the trial step is computed by freezing of the plastic flow during the time interval ΔT between the times t_n and t_{n+1}. Within the plastic corrector step, the right Cauchy-Green tensor $\mathbf{C}$ is held fixed while the internal variables are updated so as to fulfill the constitute law.

The understanding that the unimodular tensor $\mathbf{F}_{\mathbf{p}}$ is an element of the Lie group $SL^{+}(3,\mathbb{R}^3)$, while $\mathbf{L}_{\mathbf{p}}$ is an element of the corresponding Lie algebra, motivates the use of the exponential map for time integration

$$\mathbf{F}_{\mathbf{p}}^{-1}|_{n+1} = \exp(-\Delta T\,\mathbf{L}_{\mathbf{p}})\mathbf{F}_{\mathbf{p}}^{-1}|_{n}, \tag{60}$$

where $\mathbf{F}_{\mathbf{p}}^{-1}|_{n+1}$ and $\mathbf{F}_{\mathbf{p}}^{-1}|_{n}$ are plastic parts of the deformation gradient at the time step t_{n+1} and t_n. By this equation the condition of plastic incompressibility is preserved exactly. The evaluation of the exponential map is

carried out using an algorithm for non-symmetric arguments given in Sansour and Kollmann (1998). The corresponding derivatives are computed following a suggestion in Sansour and Wagner (2001). The elastic strain measure $\mathbf{C}\mathbf{C}_\mathbf{p}^{-1}$ at time step t_{n+1} is expressed by

$$\mathbf{C}\mathbf{C}_\mathbf{p}^{-1}\mid_{n+1} = \mathbf{C}\mid_{n+1} \exp(-\Delta T \mathbf{L}_\mathbf{p}) \mathbf{C}_\mathbf{p}^{-1}\mid_n \exp(-\Delta T \mathbf{L}_\mathbf{p}^{\mathrm{T}}) \tag{61}$$

and the isotropic hardening variable is updated according to

$$Z\mid_{n+1} = Z\mid_n + \sqrt{\frac{2}{3}} \Delta T \lambda|_{n+1}. \tag{62}$$

Plastic multiplier at the time step t_{n+1} is defined as

$$\lambda|_{n+1} = \lambda|_n + \Delta\lambda. \tag{63}$$

In order to obtain the increment of the plastic multiplier $\Delta\lambda$, the yield function (55) and the evolution equation (53) are used

$$\mathbf{L}_\mathbf{p} = \lambda \frac{\operatorname{dev} \mathbf{\Gamma}^{\mathrm{T}}}{\| \operatorname{dev} \mathbf{\Gamma} \|}, \tag{64}$$

$$f(\lambda, \mathbf{L}_\mathbf{p}) = \| \operatorname{dev} \mathbf{\Gamma} \| - \sqrt{\frac{2}{3}} (\sigma_Y + Y) = 0, \tag{65}$$

$$Y(\lambda) = -HZ\mid_{n+1} - (\sigma_\infty - \sigma_Y)\left(1 - \exp\left(-\eta Z\mid_{n+1}\right)\right). \tag{66}$$

By inserting the update relations of the state variables in the yield function, a non-linear scalar equation for the plastic multiplier is obtained which has to be solved employing Newton's iterative solution procedure

$$\frac{\partial f}{\partial \lambda} \cdot \Delta\lambda = -f. \tag{67}$$

The derivative $\partial f / \partial \lambda$ is solved with the well-known chain rule

$$\frac{\partial f}{\partial \lambda} = \frac{\partial(\| \operatorname{dev} \mathbf{\Gamma} \|)}{\partial(\operatorname{dev} \mathbf{\Gamma})} \frac{\partial(\operatorname{dev} \mathbf{\Gamma})}{\partial \mathbf{\Gamma}} \frac{\partial \mathbf{\Gamma}}{\partial \lambda} - \sqrt{\frac{2}{3}} \frac{\partial Y}{\partial \lambda}. \tag{68}$$

In what follows, the computations are carried out using a notation with explicit reference to indices. The first two terms are

$$\frac{\partial(\| \operatorname{dev} \mathbf{\Gamma} \|)}{\partial(\operatorname{dev} \Gamma)_a{}^b} = \frac{(\operatorname{dev} \Gamma)^a{}_b}{\| \operatorname{dev} \Gamma \|}, \tag{69}$$

$$\frac{\partial(\operatorname{dev} \Gamma)_a{}^b}{\partial \Gamma_c{}^d} = \delta_a{}^c \delta^b{}_d - \frac{1}{3} \delta^c{}_d \delta_a{}^b \tag{70}$$

and the third is

$$\frac{\partial Y(\lambda)}{\partial \lambda} = -\sqrt{\frac{2}{3}} \Delta T \left[H + \eta (\sigma_\infty - \sigma_Y) \exp\left(-\eta Z\mid_{n+1}\right)\right]. \tag{71}$$

The derivative of the stress tensor with respect to the plastic multiplier results out of the equation

$$\frac{\partial \Gamma_c{}^d}{\partial \lambda} = \frac{\partial \Gamma_c{}^d}{\partial (L_p)^e{}_f} \left(\left. \frac{\partial (L_p)^e{}_f}{\partial \lambda} \right|_{explicit} + \frac{\partial (L_p)^e{}_f}{\partial \nu^g{}_h} \frac{\partial \nu^g{}_h}{\partial \Gamma_m{}^n} \frac{\partial \Gamma_m{}^n}{\partial \lambda} \right) \tag{72}$$

which gives

$$\frac{\partial \Gamma_m{}^n}{\partial \lambda} = \left(\delta_c{}^m \delta_n{}^d - \frac{\partial \Gamma_c{}^d}{\partial (L_p)^e{}_f} \frac{\partial (L_p)^e{}_f}{\partial \nu^g{}_h} \frac{\partial \nu^g{}_h}{\partial \Gamma_m{}^n} \right)^{-1} \left. \frac{\partial \Gamma_c{}^d}{\partial (L_p)^e{}_f} \frac{\partial (L_p)^e{}_f}{\partial \lambda} \right|_{explicit}. \tag{73}$$

Here, it is important to point out that 'explicit' refers to the derivative of those terms which explicitly include the quantity with respect to which the derivative is considered. Some terms in (73) read

$$\frac{\partial (L_p)^e{}_f}{\partial \nu^g{}_h} \frac{\partial \nu^g{}_h}{\partial \Gamma_m{}^n} = \frac{\lambda}{\| \operatorname{dev} \mathbf{\Gamma} \|} \left[\frac{\partial (\operatorname{dev} \Gamma)_f{}^e}{\partial \Gamma_m{}^n} - \frac{(\operatorname{dev} \Gamma)_f{}^e (\operatorname{dev} \Gamma)^u{}_v}{\| \operatorname{dev} \mathbf{\Gamma} \|^2} \frac{\partial (\operatorname{dev} \Gamma)_u{}^v}{\partial \Gamma_m{}^n} \right] \tag{74}$$

$$\left. \frac{\partial (L_p)^e{}_f}{\partial \lambda} \right|_{explicit} = \frac{(\operatorname{dev} \Gamma)_f{}^e}{\| \operatorname{dev} \mathbf{\Gamma} \|} = \nu^e{}_f. \tag{75}$$

Finally, and for the sake of brevity, the term $\partial \mathbf{\Gamma} / \partial \mathbf{L}_\mathbf{p}$ is obtained in the Appendix A:.

Now, and since all terms in (67) are obtained, the increment of the plastic multiplier $\Delta\lambda$ can be determined and the plastic multiplier at the time step t_{n+1} can be updated by equation (63). With $\Delta\lambda$ at hand, the inverse of the plastic part of deformation gradient, $\mathbf{F}_\mathbf{p}{}^{-1}$, can be updated. With the latter, all quantities given in this section can be updated as well.

4.2 Consistent elastoplastic tangent modulus

The algorithmic tangent operator is obtained by linearization of the second Piola-Kirchhoff tensor $\mathbf{S}$ with respect to the right Cauchy-Green deformation tensor. The

tensor $\mathbf{S}$ can be written as

$$\mathbf{S} = \mathbf{C}^{-1}\boldsymbol{\Xi} \ . \tag{76}$$

Accordingly, its linearization takes the following form

$$\frac{\partial \mathbf{S}}{\partial \mathbf{C}} = \frac{\partial \mathbf{C}^{-1}}{\partial \mathbf{C}}\boldsymbol{\Xi} + \mathbf{C}^{-1}\frac{\partial \boldsymbol{\Xi}}{\partial \mathbf{C}}. \tag{77}$$

Using indices, this equation can be written as

$$\frac{\partial[(C^{-1})^{ua}\Xi_a{}^b]}{\partial C_{kl}} = -(C^{-1})^{uk}(C^{-1})^{al}\Xi_a{}^b + (C^{-1})^{ua}\frac{\partial \Xi_a{}^b}{\partial C_{kl}}. \tag{78}$$

A general expression for the derivative $\partial\boldsymbol{\Xi}/\partial\mathbf{C}$ is obtained according to

$$\begin{aligned}\frac{\partial \Xi_a{}^b}{\partial C_{kl}} = \frac{\partial (\Xi^{el.})_a{}^b}{\partial (CC_p^{-1})_c{}^d}\Bigg(&\frac{\partial (CC_p^{-1})_c{}^d}{\partial C_{kl}}\Bigg|_{explicit} + \\ &\frac{\partial (CC_p^{-1})_c{}^d}{\partial (F_p^{-1})^e{}_f}\frac{\partial (F_p^{-1})^e{}_f}{\partial (L_p)^g{}_h}\frac{\partial (L_p)^g{}_h}{\partial C_{kl}}\Bigg) + \frac{\partial (\Xi^{pl.})_a{}^b}{\partial C_{kl}}\Bigg|_{explicit} \\ &+ \frac{\partial (\Xi^{pl.})_a{}^b}{\partial (F_p^{-1})^e{}_f}\frac{\partial (F_p^{-1})^e{}_f}{\partial (L_p)^g{}_h}\frac{\partial (L_p)^g{}_h}{\partial C_{kl}}.\end{aligned} \tag{79}$$

The terms $\partial(\Xi^{el.})_a{}^b/\partial(CC_p^{-1})_c{}^d$ and $\partial(CC_p^{-1})_c{}^d/\partial(F_p^{-1})^e{}_f$ are identical to the terms given Eq. (88) and Eq. (89) as derived in Appendix A:, while $\partial(F_p^{-1})^e{}_f/\partial(L_p)^g{}_h$ is given by Eq. (90). $\partial(\Xi^{pl.})_i{}^j/\partial(F_p^{-1})^c{}_d$ is formulated in Appendix B:. Further, the explicit derivatives of $\mathbf{C}\mathbf{C}_\mathbf{p}^{-1}$ and of the 'plastic' part of the stress read

$$\frac{\partial (CC_p^{-1})_u{}^v}{\partial C_{rs}}\Bigg|_{explicit} = \delta_u{}^r(F_p^{-1})^{sc}(F_p^{-1})^v{}_c, \tag{80}$$

$$\begin{aligned}\frac{\partial (\Xi^{pl.})_a{}^b}{C_{kl}}\Bigg|_{explicit} = &\frac{c}{(\det F_p^{-1}\,|_n)^{2/3}} \\ &\Big[\delta_a{}^k(F_p^{-1})^l{}_n(C^{-1})^{no}(F_p^{-1})^b{}_o - \\ &C_{am}(F_p^{-1})^m{}_n(C^{-1})^{nk}(C^{-1})^{ol}(F_p^{-1})^b{}_o \\ &-(F_p^{-1})^k{}_a(F_p^{-1})^l{}_o(C^{-1})^{ob} + \\ &(F_p^{-1})^m{}_a C_{mn}(F_p^{-1})^n{}_o(C^{-1})^{ok}(C^{-1})^{bl}\Big].\end{aligned} \tag{81}$$

It should be noted that in equation (81) we use characteristic

$$\frac{c}{(\det \mathbf{F}_\mathbf{p}^{-1}\,|_n)^{2/3}} = \frac{c}{(\det \mathbf{F}_\mathbf{p}^{-1}\,|_{n+1})^{2/3}}.$$

The determination of $\partial(L_p)^g{}_h/\partial C_{kl}$ is carried out using the following two equations

$$\frac{\partial (L_p)^i{}_j}{\partial C_{kl}} = \frac{\partial (L_p)^i{}_j}{\partial \lambda}\frac{\partial \lambda}{\partial C_{rs}} + \frac{\partial (L_p)^i{}_j}{\partial \nu^a{}_b}\frac{\partial \nu^a{}_b}{\partial C_{rs}}, \tag{82}$$

$$\frac{\partial \nu^a{}_b}{\partial C_{rs}} = \frac{\partial \nu^a{}_b}{\partial \Gamma_c{}^d}\left[\frac{\partial \Gamma_c{}^d}{\partial C_{rs}}\Bigg|_{explicit} + \frac{\partial \Gamma_c{}^d}{\partial (L_p)^e{}_f}\frac{\partial (L_p)^e{}_f}{\partial C_{rs}}\right]. \tag{83}$$

Inserting Eq. (82) in Eq. (83) gives

$$\begin{aligned}\frac{\partial \nu^a{}_b}{\partial C_{rs}} = \frac{\partial \nu^a{}_b}{\partial \Gamma_c{}^d}\Bigg[&\frac{\partial \Gamma_c{}^d}{\partial C_{rs}}\Bigg|_{explicit} + \frac{\partial \Gamma_c{}^d}{\partial (L_p)^e{}_f} \\ &\left(\frac{\partial (L_p)^e{}_f}{\partial \lambda}\frac{\partial \lambda}{\partial C_{rs}} + \frac{\partial (L_p)^e{}_f}{\partial \nu^g{}_h}\frac{\partial \nu^g{}_h}{\partial C_{rs}}\right)\Bigg].\end{aligned} \tag{84}$$

The use of von Mises flow rule $\| \operatorname{dev} \boldsymbol{\Gamma} \| - \sqrt{\frac{2}{3}}(\sigma_Y - Y) = 0$ gives

$$\begin{aligned}\frac{\partial \lambda}{\partial C_{rs}} = &\frac{1}{\sqrt{\frac{2}{3}}\frac{\partial Y}{\partial \lambda} - \frac{\partial \| \operatorname{dev} \boldsymbol{\Gamma} \|}{\partial \lambda}} \\ &\Bigg[\frac{\partial (\| \operatorname{dev} \boldsymbol{\Gamma} \|)}{\partial (\operatorname{dev} \Gamma)_a{}^b}\frac{\partial (\operatorname{dev} \Gamma)_a{}^b}{\partial \Gamma_c{}^d}\frac{\partial \Gamma_c{}^d}{\partial (L_p)^e{}_f}\frac{\partial (L_p)^e{}_f}{\partial \nu^g{}_h}\frac{\partial \nu^g{}_h}{\partial C_{rs}} \\ &+ \frac{\partial (\| \operatorname{dev} \boldsymbol{\Gamma} \|)}{\partial (\operatorname{dev} \Gamma)_a{}^b}\frac{\partial (\operatorname{dev} \Gamma)_a{}^b}{\partial \Gamma_c{}^d}\frac{\partial \Gamma_c{}^d}{\partial C_{rs}}\Bigg|_{explicit}\Bigg],\end{aligned} \tag{85}$$

which is to be inserted in (84). The resulting equation can be solved for $\partial\nu^a{}_b/\partial C_{rs}$, which results in

$$\begin{aligned}\frac{\partial \nu^g{}_h}{\partial C_{rs}} = &\Bigg[\delta_g{}^a\delta^h{}_b - \frac{\partial \nu^a{}_b}{\partial \Gamma_c{}^d}\frac{\partial \Gamma_c{}^d}{\partial (L_p)^e{}_f} \\ &\Bigg(\frac{\partial (L_p)^e{}_f}{\partial \lambda}\frac{1}{\sqrt{\frac{2}{3}}\frac{\partial Y}{\partial \lambda} - \frac{\partial (\| \operatorname{dev} \boldsymbol{\Gamma} \|)}{\partial \lambda}}\frac{\partial (\| \operatorname{dev} \boldsymbol{\Gamma} \|)}{\partial (\operatorname{dev} \Gamma)_p{}^q} \\ &\frac{\partial (\operatorname{dev} \Gamma)_p{}^q}{\partial \Gamma_u{}^v}\frac{\partial \Gamma_u{}^v}{\partial (L_p)^x{}_y}\frac{\partial (L_p)^x{}_y}{\partial \nu^g{}_h} - \frac{\partial (L_p)^e{}_f}{\partial \nu^g{}_h}\Bigg)\Bigg]^{-1} \\ &\Bigg(\frac{\partial \nu^a{}_b}{\partial \Gamma_c{}^d}\frac{\partial \Gamma_c{}^d}{\partial (L_p)^e{}_f}\frac{\partial (L_p)^e{}_f}{\partial \lambda}\frac{1}{\sqrt{\frac{2}{3}}\frac{\partial Y}{\partial \lambda} - \frac{\partial (\| \operatorname{dev} \boldsymbol{\Gamma} \|)}{\partial \lambda}} \\ &\frac{\partial (\| \operatorname{dev} \boldsymbol{\Gamma} \|)}{\partial (\operatorname{dev} \Gamma)_p{}^q}\frac{\partial (\operatorname{dev} \Gamma)_p{}^q}{\partial \Gamma_u{}^v} + \frac{\partial \nu^a{}_b}{\partial \Gamma_u{}^v}\Bigg)\frac{\partial \Gamma_u{}^v}{\partial C_{rs}}\Bigg|_{explicit}\end{aligned} \tag{86}$$

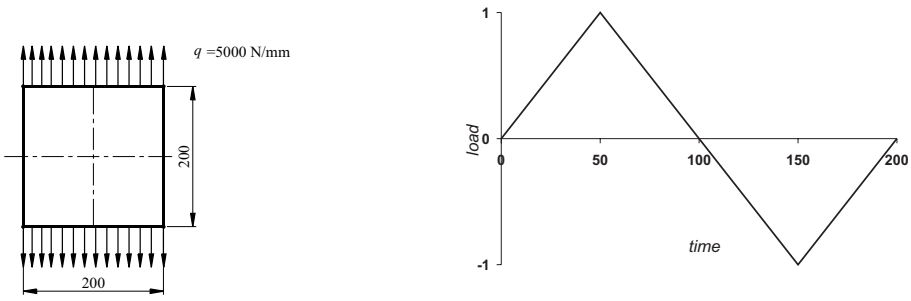

Figure 1 : Membrane: geometry and load mode diagram

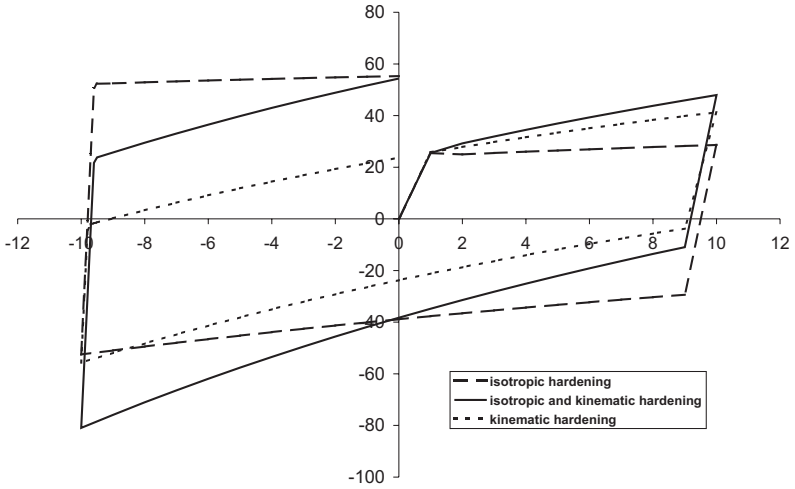

Figure 2 : Membrane: load deflection curves for different type of hardening

which can be inserted in (85) and in (82). Having established the expressions for $\partial \nu^a{}_b / \partial C_{rs}$ and $\partial \lambda / \partial C_{rs}$, Eq. (82) can be inserted in (79) which results in the exact expression for the consistent elastoplastic tangent operator as formulated in Eq. (78).

It should be stressed that the resulting expression for the tangent operator is not symmetric. The expression is quite involved. This fact is simply a result of the multiplicative structure of the theory which has its roots in the multiplicative decomposition of the deformation gradient itself.

5 Numerical examples

The integration algorithms presented have been implemented in a code for shell finite element computations. The shell theory and the finite element itself have been presented in previous publications in Sansour and Kollmann (1998) and Sansour and Wagner (2001).

The shell formulation is based on a 7-parameter theory which includes transversal strains and thus enables the application of a complete three-dimensional constitutive law. The enhanced strain concept is applied to avoid locking phenomena.

5.1 Uniaxially loaded membrane

The first example is a thin plate under in-plane line loading, Fig. 1. Due to symmetry conditions only one quarter of the membrane is discretized with 1 element. The geometry of the plate is given in Fig. 1. The material data are as follows: Young's modulus $E = 210 \times 10^3$ N/mm^2, Poisson's ratio $\nu = 0.3$, the initial yield stress $\sigma_Y = 240$ N/mm^2, the isotropic hardening parameter $H = 8.0 \times 10^2$ N/mm^2 and the kinematic hardening parameter $c = 8.0 \times 10^2$ N/mm^2. The plate is subjected to a line load of $q = 5000$ N/mm and a loading cycle as presented in Fig. 1.

The load factor versus displacement curves is plotted in Fig. 2 for isotropic, kinematic and a combined isotropic

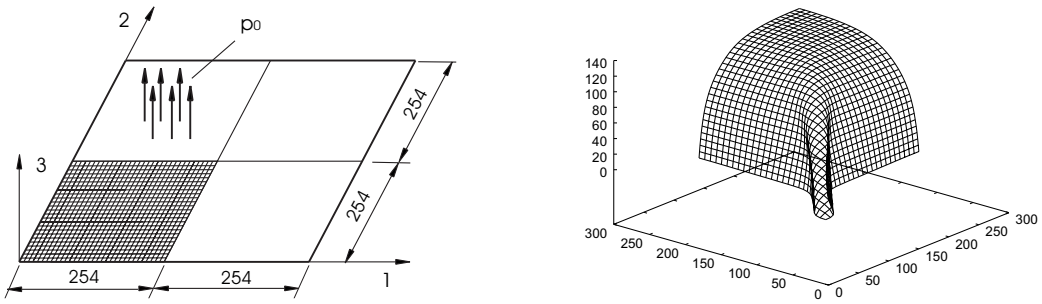

Figure 3 : Square plate: geometry and deformed configuration at $u_3 = 140$ mm

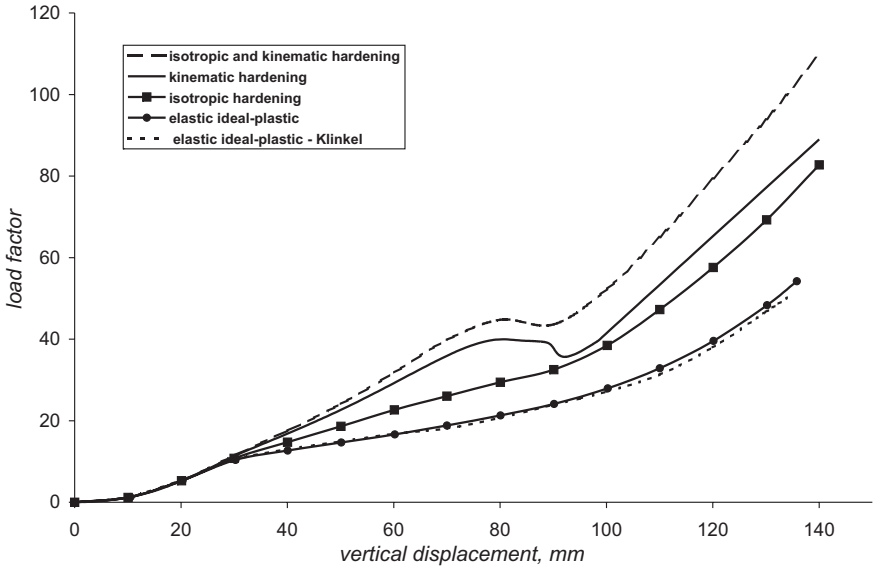

Figure 4 : Square plate: load deflection curves for the center point

and kinematic hardening cases. From the figure the influence of kinematic hardening is clearly demonstrated.

5.2 Simply supported plate

The deformation of a simply supported square plate, depicted in Fig. 3, is considered. The length of the plate is $2L = 508$ mm and the thickness is $h_0 = 2.54$ mm. The material data are as follows: Young's modulus $E = 69 \times 10^3$ N/mm^2, Poisson's ratio $\nu = 0.3$, the initial yield stress $\sigma_Y = 248$ N/mm^2, the isotropic hardening parameter $H = 3.0 \times 10^3$ N/mm^2 and the kinematic hardening parameter $c = 3.0 \times 10^3$ N/mm^2. The plate is subjected to the conservative load of $p_0 = 10^{-2}$ N/mm^2. Due to symmetry only one quarter of the plate is dicretized by 32×32 elements.

The load versus vertical displacement at the center point is plotted in Fig. 4. In this figure, the curve computed by the proposed formulation employing combined isotropic ($H = 3.0 \times 10^3$ N/mm^2) and kinematic hardening ($c = 3.0 \times 10^3$ N/mm^2) is compared with those obtained by the use of only isotropic hardening ($H = 3.0 \times 10^3$ N/mm^2) or by the elastic-ideal-plastic case. As may be seen, the influence of the kinematic hardening on the deformation response is significant. A full agreement of the load displacement curve obtained for an elastic ideal-plastic material behaviour with that published in Klinkel (2000) is evident; in the large strain range small deviations are expected due to the fact that the employed elastic constitutive law is different.

5.3 Scordelis-Lo roof

A Scordelis-Lo roof subjected to gravity loading is considered next. Both straight longitudinal edges are free, and diaphragms, that suppress any movement in direction

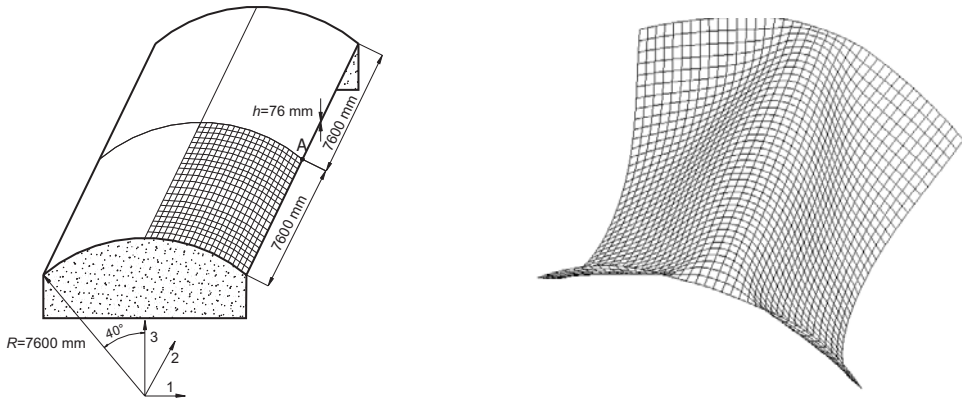

Figure 5 : Scordelis-Lo roof: geometry and deformed configuration at $u_3 = 140$ mm

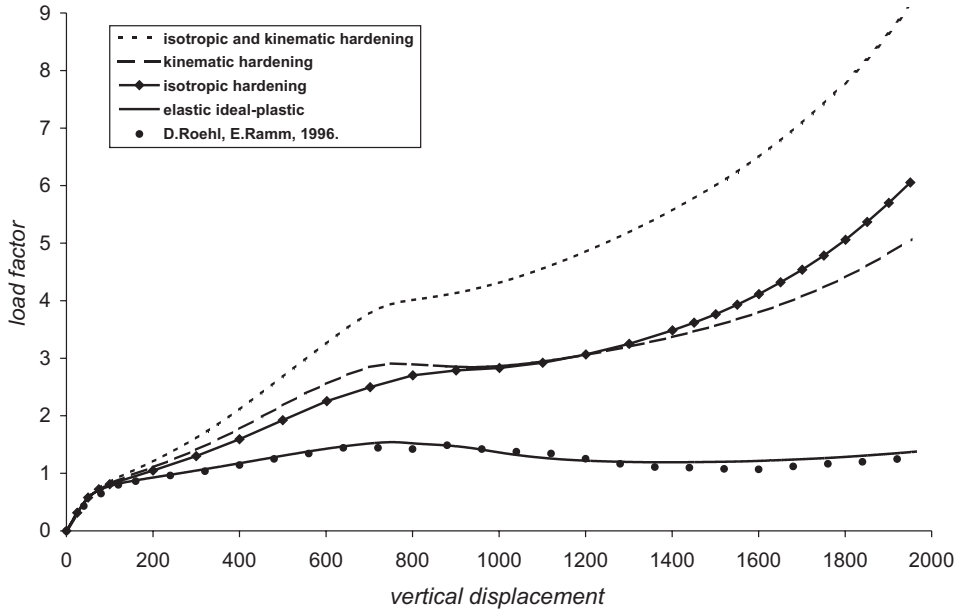

Figure 6 : Scordelis-Lo roof: load deflection curves for the point A

1 and 3, support two circular edges. Because of the symmetry, only one-quarter of the roof has been discretized by 20×20 elements. The half-length is $L = 7600$ mm, the radius is $R = 7600$ mm and the thickness is $h = 0.076$ mm. The material properties are: elastic modulus is $E = 210000$ N/mm^2, Poisson's ratio $\nu = 0.0$, the yield stress $\sigma_Y = 4.2$ N/mm^2, the isotropic hardening parameter $H = 0.8$ kN/mm^2 and kinematic hardening parameter $c = 0.4$ kN/mm^2. The value of the reference gravity load is $q_0 = 4.0 \times 10^{-3}$ N/mm^2. The curve for the elastic ideal-plastic case is compared with the one obtained in Roehl and Ramm (1996). Excellent agreement is observed.

5.4 Hemispherical shell subjected to line load

As next example, a hemispherical shell with a central opening 30° is considered. The shell is clamped along the bottom end, and axial displacement and rotations are allowed on the upper boundary. A line load with reference value of $q_0 = 10$ N/mm is applied at the upper boundary. The loading, geometry and finite mesh are shown in Fig. 7. The computation is performed for elastic ideal-plastic case, isotropic hardening, kinematic hardening and combined isotropic and kinematic hardening. The material data are: Young's modulus $E = 212$ GPa, Poisson's ratio $\nu = 0.2581$, the initial yield stress $\sigma_Y = 243$ MPa

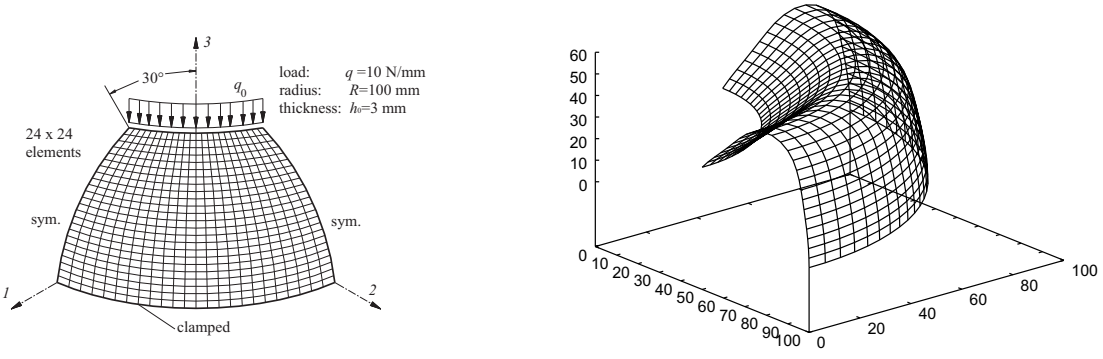

Figure 7 : Hemispherical shell: geometry and deformed configuration

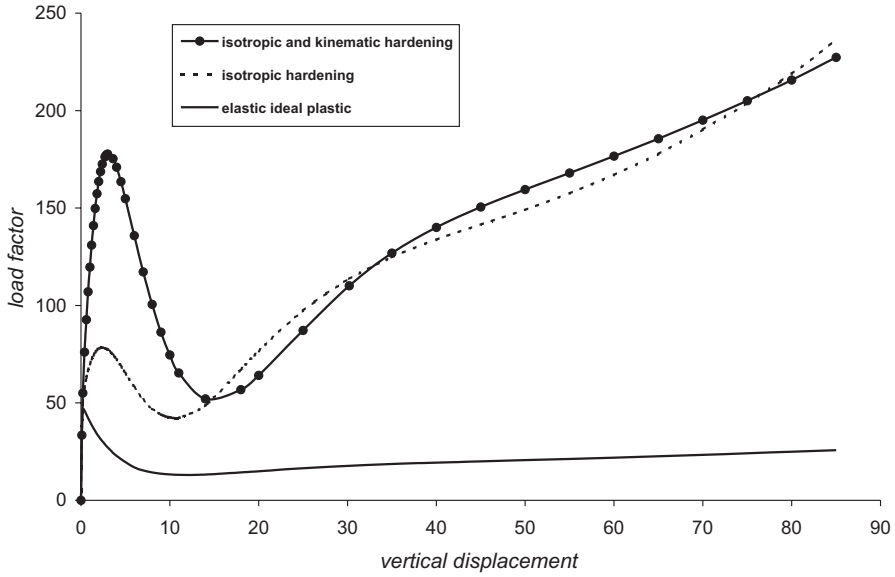

Figure 8 : Hemispherical shell: load deflection curves

and the kinematic and isotropic hardening parameters are $c = 0.1 \times E$ and $H = 0.1 \times E$. A diagram showing the load factor versus the vertical displacement at the upper boundary is plotted in Fig. 8. The Figure shows the great influence of the hardening parameters on the deformation, especially when combined isotropic and kinematic hardening are considered.

6 Conclusion

In this paper a theoretical framework for a free energy-based formulation of the kinematic hardening is developed. In addition, numerical schemes has been addressed in detail. An efficient numerical model for large strain elastoplastic material response has been presented. The material model employs the von Mises yield criterion with combined isotropic and free energy-based kinematic hardening. The integration algorithm, based on the multiplicative decomposition of the deformation gradient, employs the predictor-corrector method. The derived back stress tensor shows some advantages, in comparison with relations available in literature. In contrast to a rate formulation, here the symmetric back stress tensor is defined by relations automatically obeying the objectivity condition. The constitutive equations are written in terms of the spatial quantities: the Kirchhoff stress tensor and the left Cauchy-Green deformation tensor, while the local integration algorithm and the consistent elastoplastic tangent modulus are considered at the reference configuration. The applied consistent elastoplastic tangent modulus ensures high convergence rate in global solution

procedures. The numerical example shows robustness, and numerical efficiency of the proposed computational procedure.

Acknowledgement: This study is the result of research done at the Institute for Structural Analysis of the University of Karlsruhe. The authors express their gratitude to Prof. Dr. Werner Wagner, Head of the Institute. Financial support of the Alexander von Humboldt Foundation is gratefully acknowledged.

Appendix A: The Derivative of the relative stress $\mathbf{\Gamma}$ with respect to the plastic rate $\mathbf{L_p}$

This derivative is established using the chain rule:

$$\frac{\partial \Gamma_i{}^j}{\partial (L_p)^k{}_l} = \frac{\partial (\Gamma^{el.})_i{}^j}{\partial (CC_p^{-1})_a{}^b} \frac{\partial (CC_p^{-1})_a{}^b}{\partial (F_p^{-1})^c{}_d} \frac{\partial (F_p^{-1})^c{}_d}{\partial (L_p)^k{}_l} + + \frac{\partial ((\Gamma^{pl.})_i{}^j)}{\partial (F_p^{-1})^c{}_d} \frac{\partial (F_p^{-1})^c{}_d}{\partial (L_p)^k{}_l}. \tag{87}$$

In the following we provide expressions to each single term involved. We make use of equation (58) to get

$$\frac{\partial (\Gamma^{el.})_i{}^j}{\partial (CC_p^{-1})_a{}^b} = 2\rho_0 \Big\{ \alpha_1 [\delta^a{}_b (CC_p^{-1})_i{}^j + ((CC_p^{-1})_r{}^r - 3)\delta_i{}^a \delta^j{}_b] + + \alpha_2 [\delta_i{}^a (CC_p^{-1})_b{}^j + ((CC_p^{-1})_i{}^a - \delta_i{}^a)\delta^j{}_b] \Big\}. \tag{88}$$

Further, we have

$$\frac{\partial (CC_p^{-1})_a{}^b}{\partial (F_p^{-1})^c{}_d} = C_{ac} (F_p^{-1})^{bd} + C_{au} (F_p^{-1})^{ud} \delta^b{}_c, \tag{89}$$

as well as

$$\frac{\partial (F_p^{-1})^c{}_d}{\partial (L_p)^k{}_l} = \frac{\partial (F_p^{-1})^c{}_d}{\partial [\exp(-\Delta T L_p)]^e{}_f} \frac{\partial [\exp(-\Delta T L_p)]^e{}_f}{\partial (-\Delta T L_p)^g{}_h} \frac{\partial (-\Delta T L_p)^g{}_h}{\partial (L_p)^k{}_l}. \tag{90}$$

The first term in the last equation is elaborated by the use of Eq. (60)

$$\frac{\partial (F_p^{-1})^c{}_d}{\partial [\exp(-\Delta T L_p)]^e{}_f} = (F_p^{-1}|_n)^f{}_d \delta^c{}_e. \tag{91}$$

The second term includes the tangent of the exponential map with respect to its argument, a fourth order tensor. We consider an expression derived in Sansour and Wagner (2001) which is denoted by **DEX**. Altogether one has

$$\frac{\partial (F_p^{-1})^c{}_d}{\partial (L_p)^k{}_l} = -\Delta T (DEX)^c{}_{fk}{}^l (F_p^{-1}|_n)^f{}_d. \tag{92}$$

Finally, using Eq. (59) we derive

$$\frac{\partial (\Gamma^{pl.})_i{}^j}{\partial (F_p^{-1})^c{}_d} = \frac{c}{(\det F_p^{-1}|_n)^{2/3}} \frac{\partial \mathrm{dev}\,[C_{ia} (F_p^{-1})^a{}_b (C^{-1})^{bc} (F_p^{-1})^j{}_c]}{\partial [C_{ia} (F_p^{-1})^a{}_b (C^{-1})^{bc} (F_p^{-1})^j{}_c]} [C_{ic} (C^{-1})^{do} (F_p^{-1})^j{}_o - C_{im} (F_p^{-1})^m{}_n (C^{-1})^{nd} \delta^j{}_c], \tag{93}$$

where is the first derivative made in the same manner as in Equation (70).

Appendix B: Derivative of the stress tensor $\mathbf{\Xi}^{pl.}$ with respect to the plastic part of deformation gradient $\mathbf{F_p^{-1}}$

First, we consider the derivative of the back stress, defined in Eq. (57), with respect to

$$\frac{\partial Q_i{}^j}{\partial (F_p^{-1})^c{}_d} = \frac{c}{(\det F_p{}^{-1}|_n)^{2/3}} \frac{\partial \mathrm{dev}\,[(F_p^{-1})^a{}_i C_{ab} (F_p^{-1})^b{}_c (C^{-1})^{cj}]}{\partial [(F_p^{-1})^a{}_i C_{ab} (F_p^{-1})^b{}_c (C^{-1})^{cj}]} [\delta_i{}^l C_{kn} (F_p^{-1})^n{}_o (C^{-1})^{oj} + (F_p^{-1})^m{}_i C_{mk} (C^{-1})^{lj}] \tag{94}$$

We recall the relation defined in (51)

$$\mathbf{\Xi}^{pl.} = \mathbf{\Gamma}^{pl.} + \mathbf{Q}. \tag{95}$$

The derivative of the stress tensor $\mathbf{\Xi}$ with respect to plastic part of deformation gradient $\mathbf{F_p^{-1}}$ is then given as:

$$\frac{\partial (\Xi^{pl.})_i{}^j}{\partial (F_p^{-1})^c{}_d} = \frac{\partial (\Gamma^{pl.})_i{}^j}{\partial (F_p^{-1})^k{}_l} + \frac{\partial Q_i{}^j}{\partial (F_p^{-1})^c{}_d}. \tag{96}$$

Whereas the first term of the right hand side is already given in Eq. (93), the second is included in Eq. (94).

References

Atluri, S. N. (1984a): Alternate stress and conjugate strain measures, and mixed variational formulations involving rigid rotations, for computational analyses of finitely deformed plates and shells: Part-I: Theory. *Computers & Structures*, vol. 18, no. 1, pp. 93–116.

Atluri, S. N. (1984b): On constitutive relations at finite strain: hypo-elasticity with isotropic or kinematic hardening. *Comp. Meth. Appl. Mech. Engrg.*, vol. 43, pp. 137–171.

Başar, Y.; Itskov, M. (1999): Constitutive model and finite element formulation for large strain elasto-plastic analysis of shells. *Computational Mechanics*, vol. 23, pp. 466–481.

Dogui, A.; Sidoroff, F. (1985): Kinematic hardening in large elastoplastic strain. *Engineering Fracture Mechanics*, vol. 21, pp. 685–695.

Eterovic, A. L.; Bathe, K.-J. (1990): A hyperelastic-based large strain elasto-plastic constitutive formulation with combined isotropic-kinematic hardening using the logaritmic stress and strain measures. *Int. J. Num. Meth. Engrg.*, vol. 30, pp. 1099–1114.

Im, S.; Atluri, S. N. (1987): A study of two finite strain plasticity models: an internal time theory using Mandel's director concept and combined isotropic-kinematic hardening theory. *Int. J. Plasticity*, vol. 3, pp. 163–191.

Klinkel, S. (2000): Theorie und numerik eines volumen-elementes bei finiten elastischen und plastischen verzerrungen. *Dissertation, Universität Karlsruhe, Institut für Baustatik.*

Liu, C.-S.; Chang, C. W. (2004): Lie group symmetry applied to the computation of convex plasticity constitutive equation. *CMES: Computer Modeling in Engineering & Sciences*, vol. 6, pp. 277–294.

Maugin, G. A. (1994): Eshelby stress in elastoplasticity and ductile fracture. *Int. Journal of Plasticity*, vol. 10, pp. 393–408.

Nguyen, Q. S. (1993): Bifurcation and stability of time-independent standard dissipative systems. *In Q.S. Nguyen, editor, CISM Courses and Lectures No. 327 : Bifurcation and Stability of Dissipative Systems, Springer-Verlag*.

Papadopoulos, P.; Lu, J. (1997): A general framework for the numerical solution of problems in finite elasto-plasticity. *Comp. Meth. Appl. Mech. Engrg.*, vol. 159, pp. 1–18.

Perić, D.; Owen, D. R. J.; Honnor, M. E. (1992): A model for finite strain elasto-plasticity based on logarithmic strains: Computational issues. *Comp. Meth. Appl. Mech. Engrg.*, vol. 94, pp. 35–61.

Reed, K. W.; Atluri, S. N. (1985): Constitutive modeling and computational implementation in finite strain plasticity. *International Journal of Plasticity*, vol. 1, pp. 63–87.

Roehl, D.; Ramm, E. (1996): Large elasto-plastic finite element analysis of solids and shells with the enhanced assumed strain concept. *Int. J. Solids Structures*, vol. 33, pp. 3215–3237.

Rouainia, M.; Perić, D. (1998): A computational model for elasto-viscoplastic solids at finite strain with reference to thin shell applications. *Int. J. Num. Meth. Engrg.*, vol. 42, pp. 289–311.

Sansour, C. (2001): On the dual variable of the logarithmic strain tensor, the dual variable of the Cauchy stress tensor, and related issues. *Intenational Journal of Solids and Structures*, vol. 38, pp. 9221–9232.

Sansour, C.; Kollmann, F. G. (1998): Large viscoplastic deformation of shells. Theory and finite element formulation. *Computational Mechanics*, vol. 21, pp. 512–525.

Sansour, C.; Wagner, W. (2001): A model of finite strain viscoplasticity based on unified constitutive equations. Theoretical and computational considerations with applications to shells. *Comp. Meth. Appl. Mech. Engrg.*, vol. 191, pp. 423–450.

Sansour, C.; Wagner, W. (2003): Viscoplasticity based on additive decomposition of logaritmic strain and unified constitutive equations. Theoretical and computational considerations with reference to shell applications. *Computers and Structures*, vol. 81, pp. 1583–1594.

Simo, J. C. (1988): A frame work for finite strain elasto-plasticity based on maximum plastic dissipation and multiplicative decomposition: Part I. Continuum formulation. *Comp. Meth. Appl. Mech. Engrg.*, vol. 66, pp. 199–219.

Sorić, J.; Skoko, J.; Eckstein, A. (2002): On numerical modeling of combined isotropic-kinematic hardening at large strain elastoplasticity. *Proceedings of the Fifth World Congress on Computational Mechanics (WCCM V), Vienna University of Technology*.

Tsakmakis, C. (1996): Kinematic hardening rules in finite plasticity. Part I: A constitutive approach. *Continuum Mech. Thermodyn.*, vol. 8, pp. 215–231.

Tsakmakis, C.; Willuweit, A. (2004): A comparative study of kinematic hardening rules at finite deformations. *Int. J. of Non-linear Mech.*, vol. 39, pp. 539–554.

Wang, L. H.; Atluri, S. N. (1994): An analysis of an explicit algorithm and the radial return algorithm, and a proposed modification, in finite plasticity. *Computational Mechanics*, vol. 3, pp. 380–389.